Electronic Supplementary Material (ESI) for Soft Matter.
This journal is © The Royal Society of Chemistry 2020

Electronic Supplementary Information: Single chain in mean field simulation of flexible and semiflexible polymers: Comparison with discrete chain self-consistent field theory

So Jung Park and Jaeup U. Kim*

Department of Physics, School of Natural Science,

Ulsan National Institute of Science and Technology (UNIST), Ulsan 44919, Republic of Korea

A. Free energies of block copolymer lamellae with FJC model

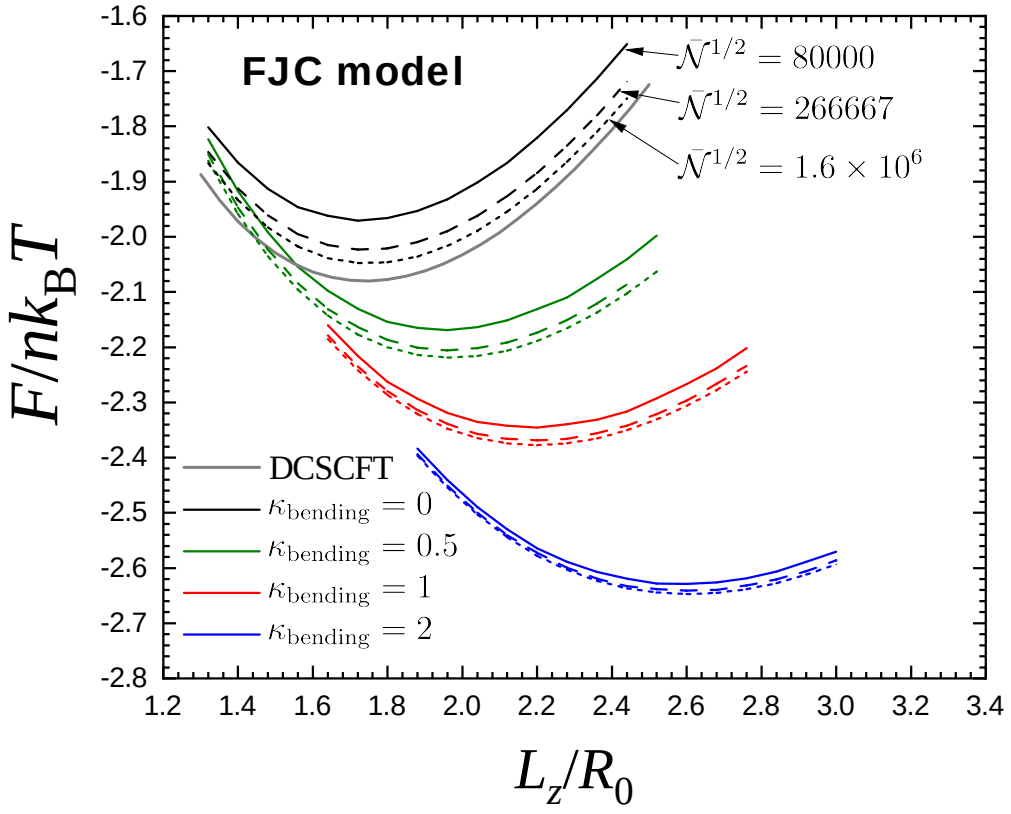

Figure S1: Free energy calculated by SCMF simulation of AB diblock copolymers in bulk lamellar phase ($\chi N = 25$, $\kappa N = 50$, $N = 14$ and $\Delta L = 0.04R_0$) modeled by FJC at different $\bar{N}$ and stiffness parameter $\kappa_{\mathrm{bending}}$. DCSCFT result of flexible FJC model is plotted with a gray line.

*Electronic address: jukim@unist.ac.kr

B. Total density distribution of compressible homopolymer melts confined between two neutral hard walls

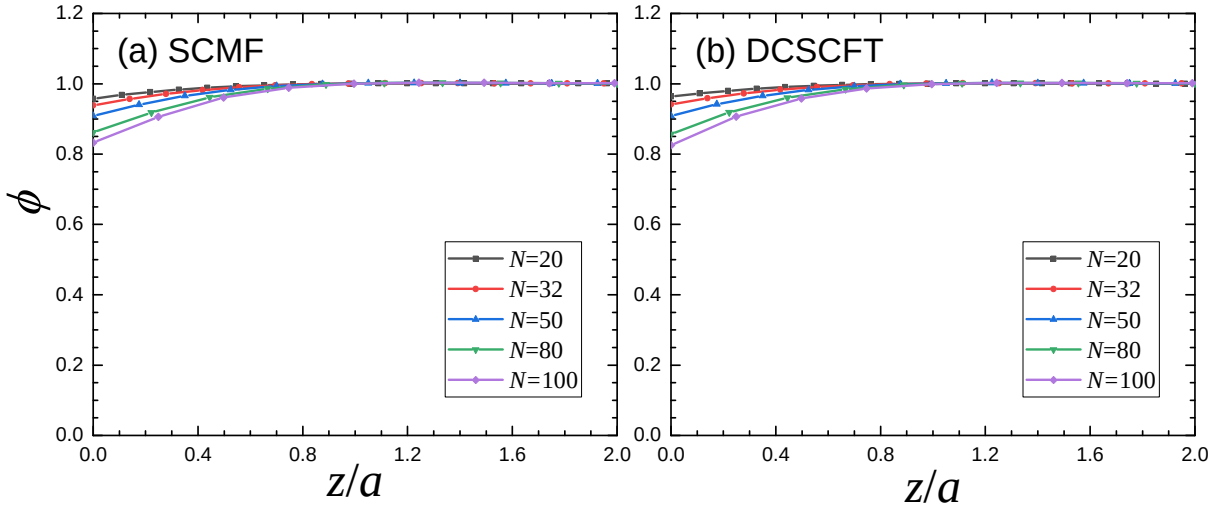

Figure S2: (a) Ensemble-averaged total density of homopolymer melts near neutral hard wall (at $z = 0$) calculated by SCMF simulation with flexible BS chain model of discrete N segments. (b) The same plot obtained from DCSCFT calculation. The compressibility is very small for both calculations, $\kappa N = 500$.

C. Self-consistent equations and free energy of FRI-DCSCFT

In this section, we present self-consistent equations and free energy expression of DCSCFT adopting finite-range interaction (FRI) for compressible AB block copolymer melts. FRI between nonbonded segments can be incorporated in DCSCFT by modifying the Hamiltonian for nonbonded interaction $\mathcal{H}_{nb}$ in eqn (4) as explained in section 3.2 in the main text.

With the modification of $\mathcal{H}_{nb}$ by eqn (29), the field theoretical transformation and saddle point approximation are still straightforward, and the self-consistent field equations are given as follows

$$\begin{aligned} w_A(\mathbf{r}) =& \frac{\chi N}{2} \int d\mathbf{R} u(\mathbf{R}) \left(\phi_B(\mathbf{r}-\mathbf{R}) - \phi_A(\mathbf{r}-\mathbf{R})\right) \\ &+ \kappa N \int d\mathbf{R} u(\mathbf{R}) \left(\phi_A(\mathbf{r}-\mathbf{R}) + \phi_B(\mathbf{r}-\mathbf{R}) - 1\right) \end{aligned} \tag{C1}$$

$$\begin{aligned} w_B(\mathbf{r}) =& \frac{\chi N}{2} \int d\mathbf{R} u(\mathbf{R}) \left(\phi_A(\mathbf{r}-\mathbf{R}) - \phi_B(\mathbf{r}-\mathbf{R})\right) \\ &+ \kappa N \int d\mathbf{R} u(\mathbf{R}) \left(\phi_A(\mathbf{r}-\mathbf{R}) + \phi_B(\mathbf{r}-\mathbf{R}) - 1\right) \end{aligned} \tag{C2}$$

After the self-consistent mean field solution is obtained, the free energy of the system is calculated by

$$\begin{aligned} \frac{F}{nk_{\mathrm{B}}T} =& -\ln\left(\frac{Q[w_A, w_B]}{V}\right) - \frac{\chi N}{4V} \int d\mathbf{r} d\mathbf{r}' \left(\phi_A(\mathbf{r}) - \phi_B(\mathbf{r})\right) u(\mathbf{r}-\mathbf{r}') \left(\phi_A(\mathbf{r}') - \phi_B(\mathbf{r}')\right) \\ &+ \frac{\kappa N}{2V} \int d\mathbf{r} d\mathbf{r}' \ \left(\phi_A(\mathbf{r}) + \phi_B(\mathbf{r}) - 1\right) u(\mathbf{r}-\mathbf{r}') \left(\phi_A(\mathbf{r}') + \phi_B(\mathbf{r}') - 1\right) \\ &- \frac{1}{V} \int d\mathbf{r} \left(w_A(\mathbf{r})\phi_A(\mathbf{r}) + w_B(\mathbf{r})\phi_B(\mathbf{r})\right) \end{aligned} \tag{C3}$$

D. Thermodynamic integration method

Free energy difference between disordered ($\chi N = 0$) and ordered lamellar phase ($\chi N = 25$) in the SCMF simulation is calculated via thermodynamic integration along the reversible path connecting the two states, and in this section we present the details of the thermodynamic integration which mostly follows the suggestion of Müller and Daoulas. [1] In this method, ordering field is externally imposed along the reversible path, and the Hamiltonian of the system includes an additional term

$$\frac{\mathcal{H}_{\text{ext}}}{nk_{\text{B}}T} = -\frac{\lambda N}{V}\int d\mathbf{r} f_{\text{ext}}(\mathbf{r})\hat{\phi}(\mathbf{r}) \tag{D1}$$

where λN and $f_{\text{ext}}(\mathbf{r})$ are the strength and spatial variation of external ordering field, respectively, which linearly couples to the order parameter $\hat{\phi} \equiv (\hat{\phi}_A - \hat{\phi}_B)/2$. Deriving the self-consistent mean field solutions for this modified Hamiltonian, each field now includes one additional term as follows,

$$w_A(\mathbf{r}) = \frac{\chi N}{2}(\phi_B - \phi_A) + \kappa N(\phi_A + \phi_B - 1) + w_A^{\text{ext}} \tag{D2}$$

$$w_B(\mathbf{r}) = \frac{\chi N}{2}(\phi_A - \phi_B) + \kappa N(\phi_A + \phi_B - 1) + w_B^{\text{ext}} \tag{D3}$$

where

$$w_A^{\text{ext}}(\mathbf{r}) = -w_B^{\text{ext}}(\mathbf{r}) = \frac{-\lambda N f_{\text{ext}}(\mathbf{r})}{2} \tag{D4}$$

In the thermodynamic integration method, reversible path is defined along the two lines on χN-λN plane as shown in Fig. S3. In the first process, the disordered state ($\chi N = 0$) gradually changes to predefined structure by increasing the parameter λN from 0 to 25 (green line in Fig. S3) while fixing $f_{\text{ext}}(\mathbf{r})$ to be $2\phi(\mathbf{r})$ obtained at $\chi N = 25$, which is the natural way to generate the simulation results at $\chi N = 25$ by using external fields. The fields acting on each type of segment in SCMF simulation are now quasi-instantaneously updated using instantaneous densities and external fields. Eqns (26) and (27) are now modified by

$$\hat{w}_{A,m} = \frac{\chi N}{2}(\hat{\phi}_{B,m} - \hat{\phi}_{A,m}) + \kappa N(\hat{\phi}_{A,m} + \hat{\phi}_{B,m} - 1) + w_{A,m}^{\text{ext}} \tag{D5}$$

$$\hat{w}_{B,m} = \frac{\chi N}{2}(\hat{\phi}_{A,m} - \hat{\phi}_{B,m}) + \kappa N(\hat{\phi}_{A,m} + \hat{\phi}_{B,m} - 1) + w_{B,m}^{\text{ext}} \tag{D6}$$

where

$$w_{A,m}^{\text{ext}} = -w_{B,m}^{\text{ext}} = -\lambda N \hat{\phi}_m^{\text{final}} \tag{D7}$$

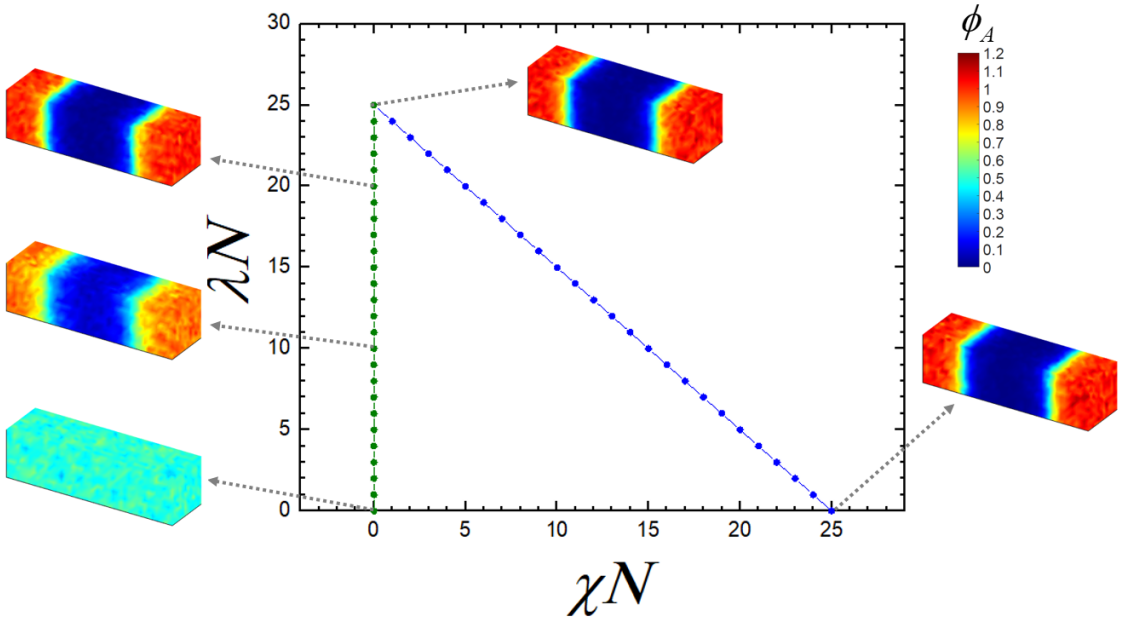

Figure S3: The reversible path adopted in thermodynamic integration scheme is illustrated on χN-λN plane with snapshots of instantaneous A segment density of each state along the reversible path.

and $\hat{\phi}_m^{\text{final}}$ is the instantaneous order parameter obtained at $\lambda N = 0$ and $\chi N = 25$.

In the second process, external fields are gradually switched off while the second control parameter χN now increases from 0 to 25 via linear path $\chi N = 25 - \lambda N$ (blue line in Fig. S3). The free energy difference between the disordered and final self-assembled phases can be calculated by adding the free energy change for each branch. Since the free energy takes the following form,

$$F = -k_{\text{B}}T \ln Z \tag{D8}$$

$$Z \propto \frac{1}{n!} \int \prod_{\alpha=1}^{n} \prod_{s\in\{0,\Delta s,\cdots,1\}} d\mathbf{r}_\alpha(s) \exp\left(-\frac{\mathcal{H}_b + \mathcal{H}_{nb} + \mathcal{H}_{\text{ext}}}{k_{\text{B}}T}\right) \tag{D9}$$

the free energy change for the first and second branches are respectively,

$$\frac{\Delta F_1}{nk_{\text{B}}T} = -\int_0^{25} d\lambda N \left\langle \frac{\Delta V_m}{V} \sum_{m=1}^{N_{\text{cell}}} f_{\text{ext},m}\hat{\phi}_m \right\rangle \Bigg|_{\chi N=0} \tag{D10}$$

$$\frac{\Delta F_2}{nk_{\text{B}}T} = -\int_{25}^{0} d\lambda N \left\langle \frac{\Delta V_m}{V} \sum_{m=1}^{N_{\text{cell}}} \left(f_{\text{ext},m}\hat{\phi}_m - \hat{\phi}_m^2\right) \right\rangle \tag{D11}$$

Here, $\langle\ \rangle$ is the ensemble average and the volume of mth cell ΔV_m is mostly $\Delta x \Delta y \Delta z$, but

factor 1/2 is multiplied if the grid point is at the neutral boundary. Throughout the paper, we evaluate the integral eqns. (D10) and (D11) by finite difference method with $\Delta(\lambda N) = 1$, after confirming that the free energy error at this step size is smaller than the accuracy required for the free energy analysis in our study.

E. Accuracy of stress calculation method

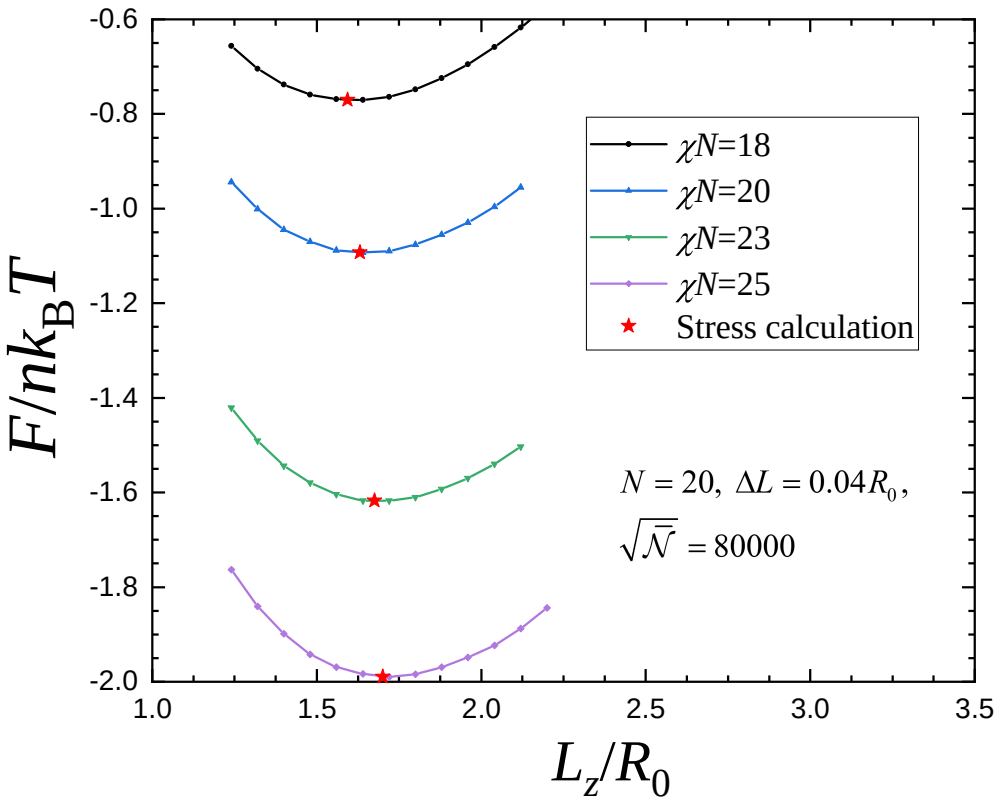

Figure S4: Free energy of symmetric ($f = 0.5$) AB block copolymer lamellar phase ($\kappa N = 50$) at various χN calculated by SCMF simulation ($N = 20$, $\Delta L = 0.04R_0$ and $\bar{N}^{1/2} = 80000$) as a function of lamellar period. The period calculated by the stress calculation method is denoted by a star in each curve.

F. $R^N_{\kappa_{\text{bending}}}$ data for BS and FJC model

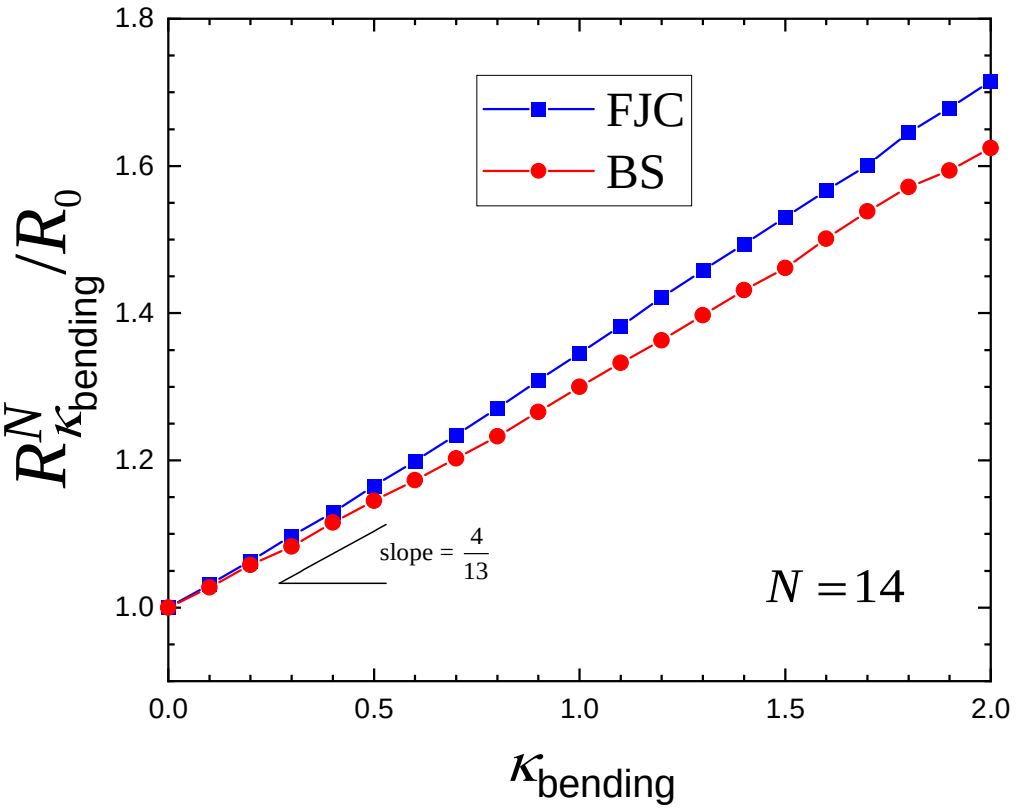

Figure S5: RMS end-to-end distance $R^N_{\kappa_{\text{bending}}}$ of the semiflexible BS and FJC model ($N = 14$) as a function of chain stiffness parameter κ_{bending}. The expected FJC slope at small κ_{bending} is shown on the graph as a guide.

For the semiflexible chain, the root-mean-square (RMS) end-to-end distance can only be calculated numerically, but at least its deviation from R_0 at small κ_{bending} can be analytically estimated. For an FJC with N segments, there exists $N-1$ bonds $\Delta\mathbf{r}_\alpha(s)$ each with length a. In the expansion of $R^2 = (\sum_s \Delta\mathbf{r}_\alpha(s))^2$, many complicated cross terms exist, but due to the assumption that κ_{bending} is small, only the dot products of neighboring $N-2$ pairs of bond vectors provide the leading order correction term which is linear in κ_{bending}. Thus, after making ensemble average, we obtain a simple formula,

$$\left\langle R^2 \right\rangle \cong (N-1)a^2 + 2a^2 \sum_{i=1}^{N-2} \langle \cos\theta_i \rangle \tag{F1}$$

where θ_i is the angle between two neighboring bond vectors as introduced in eqn (20) in the

main text. At small κ_{bending}, each average can be estimated by

$$\begin{aligned}\langle \cos\theta_i \rangle &= \int \cos\theta_i \exp\left(-\kappa_{\text{bending}}\left(1-\cos\theta_i\right)\right) d\Omega \Big/ \int \exp\left(-\kappa_{\text{bending}}\left(1-\cos\theta_i\right)\right) d\Omega \\ &\cong \frac{1}{4\pi}\int \kappa_{\text{bending}} \cos^2\theta_i d\Omega = \frac{\kappa_{\text{bending}}}{3} \end{aligned} \tag{F2}$$

Thus, $\langle R^2 \rangle \cong (N-1)a^2 + 2\kappa_{\text{bending}}(N-2)a^2/3$, and the RMS end-to-end distance in small κ_{bending} limit is obtained as,

$$R^N_{\kappa_{\text{bending}}} \cong R_0 \left[1 + \frac{N-2}{3(N-1)}\kappa_{\text{bending}}\right] \tag{F3}$$

The prefactor approaches to 1/3 in large N limit. At $N = 14$, the expected slope is $4/13 \cong 0.307$.

---

[1] M. Müller and K. C. Daoulas, *J. Chem. Phys.*, 2008, **128**, 024903.